

Non-linear density functional theory: A direct method to calculate many-electron charge densities.

Werner A. Hofer and Krisztián Palotás

Surface Science Research Centre, University of Liverpool, Liverpool L69 3BX, Britain
Donostia International Physics Center, San Sebastian, Spain

November 23, 2018

Abstract

We suggest to include the density of electron charge explicitly in the electron potential of density functional theory, rather than implicitly via exchange-correlation functionals. The advantages of the approach are conceptual and numerical. Conceptually, it allows to formulate a physical principle for the development of quantum mechanical systems: it is the principle of energetic equilibrium, because the energy principle, in this case, applies not only globally, but also on a local level. The method is an order- N method, scaling linearly with the number of atoms. It is used to calculate the electronic groundstate of a metallic surface, where we find good agreement with experimental values.

1 Density functional theory

A key innovation in theoretical solid state physics in the last fifty years was the reformulation of quantum mechanics in a density formalism, based on the Hohenberg-Kohn theorem [1]. Despite initial resistance, in particular from quantum chemists, the method has replaced previous frameworks and provides, to date, the most advanced theoretical model for the calculation of atoms, solids, and liquids. However, its implementation relies on a rather cumbersome detour. While the Hohenberg-Kohn theorem is formulated exclusively in terms of electron charge densities and energy functionals, calculations today are based almost exclusively on the specifications given by Kohn and Sham one year after the initial theorem was made public [2]. These Kohn-Sham equations define, how the electron interactions within a system can be split into three separate single-electron parts: a Coulomb potential U_{Cou} , giving the electron-ion attraction and the electron-electron repulsion; an exchange potential U_X , taking into account the Pauli exclusion principle; and a correlation potential U_C , covering

the correlated motion of electrons in a many-electron system. Then every electron in the system is described by a single-particle Schrödinger equation with the effective potential U_{eff} :

$$U_{eff} = U_{Coul} + U_X + U_C \quad (1)$$

in order to determine the charge density. Within the local density approximation, the exchange and correlation potentials are usually combined and thought to be depending on the local density of electron charge $\rho(\mathbf{r})$:

$$U_{XC}(\mathbf{r}) = U_{XC}(\rho(\mathbf{r})) \quad (2)$$

The variational problem thus contained at every single step of the energy minimization cycle a solution of the single-particle Schrödinger equation, from which the electron eigenstates and their eigenvalues are determined. The density of charge at a given step of the cycle is calculated by adding single-electron charges:

$$\rho(\mathbf{r}) = \sum_{i=1}^N \psi_i(\mathbf{r})\psi_i^*(\mathbf{r}) \quad (3)$$

N denotes the total number of electrons in the system. While this procedure is generally successful, and implemented today in numerical methods optimized for efficiency (see e.g. the ingenious way ionic and electron degrees of freedom are treated on much the same footing following a method developed by Car and Parinello [3]), it is highly inefficient in one crucial conceptual point: If, according to the Hohenberg-Kohn theorem, the density of charge is the only physically relevant variable of the system, then solving the Schrödinger equation, setting up the eigenvectors, and computing the density of electron charge is an operation, which creates a vast amount of redundant information. Every information, pertaining to the solution of the single-particle Schrödinger equation and the summation of single electron charges is discarded at the end of every step in the iteration cycle. One could therefore say that more than 90% of the information created in today's simulations is actually irrelevant. The question thus arises: *Do we have to create this information at all, or can we find a more direct way to arrive at the groundstate density of charge without this cumbersome detour via the single-particle Schrödinger equation?*

From a physical point of view, this state of affairs is easy to understand, if one considers the basic innovation, quantum mechanics introduced into the original framework of mechanics. It is the property of *phases* and *phase correlations*, which, even though it is present in any many-electron system, does not find an expression in its key quantity, the density of charge. Inducing phase correlations into density functional theory thus meant to rebuild a phase coherent system by way of the original Schrödinger equation. The easiest way to build such a system is to determine the coherent wavefunctions of single electrons and to ensure that the states are orthogonal in Hilbert space.

A more general approach would be to look at phase-correlations within a different framework. This framework, the theory of density matrices [4, 5, 6],

has consequently been the focus of research over a period of more than ten years. However, a framework combining the notion of phase-coherence for many-electron wavefunctions, and the basic requirement in DFT to find the groundstate density, has so far been missing. In this paper, we introduce such a *direct* method and show how it can be used to determine the groundstate density without any recourse to the single-particle Schrödinger equation.

The paper was written in the spirit of *orbital free* density functional theory [7, 8, 9]. It is frequently pointed out by protagonists of this line of research, that an orbital free, and Bloch-state free formulation of DFT has enormous potentials for numerical improvements. The main difference to the present framework is philosophical, rather than practical. While orbital free developments are essentially based on the Hohenberg-Kohn theorem and attempt to find a transferable formulation for the kinetic energy functional, we have analyzed the foundation of the theory itself and sought a continuous reformulation of the fundamental theory. Not least, because such a reformulation has substantial conceptual advantages, as will be shown in the following sections.

The paper is organised as follows: in section II we introduce the theoretical concept, based on a continuous generalisation of potentials in the many-electron Schrödinger equation. It is shown that the ensuing equation for the density of charge is non-linear, and that Schrödinger's equation is a zero-order approximation of the general relation. In section III we sketch the solution of the eigenvalue problem for a solid-state system. Finally, the new formulation is tested for metal surfaces in section IV.

2 Theoretical basis

The theorem of Hohenberg and Kohn elevated the density of charge to the state of a *physical* variable in many-electron systems. In addition, observations by scanning tunnelling microscopes seem to confirm that the observed structures at a surface are essentially due to the distribution of electron charge, measured with a resolution of a few picometer [10]. It is then quite astonishing to find that the electron charge has to be determined by a complicated computation process from the single electron states. We show in the following, how a representation of the system, without any reference to these states, can be constructed on the basis of Green's functions.

2.1 Green's functions and phase correlations

The Green's function of a many-electron system can be expanded into single electron states by a spectral decomposition [11, 12]:

$$G(\mathbf{r}, \mathbf{r}', z) = \sum_{i=1}^N \frac{\psi_i(\mathbf{r})\psi_i^*(\mathbf{r}')}{z - \epsilon_i} \quad (4)$$

Here, $G(\mathbf{r}, \mathbf{r}', z)$ is the many-electron Green's function of the system in a local basis, N the number of electrons, and z the complex energy parameter.

The Green's function will become its complex conjugate upon an exchange of the local coordinates:

$$G(\mathbf{r}, \mathbf{r}', z) = G^*(\mathbf{r}', \mathbf{r}, z^*) \quad (5)$$

It complies with a differential equation of the Hamiltonian in a local basis:

$$(H(\mathbf{r}, \mathbf{r}') - z)G(\mathbf{r}, \mathbf{r}', z) = -\delta(\mathbf{r} - \mathbf{r}') \quad (6)$$

Note that the Green's function of the many-electron system depends only on two local coordinates \mathbf{r} and \mathbf{r}' . We show now that this Green's function can be written as the product of the phase correlation functions $\Psi(\mathbf{r})$ and $\Psi(\mathbf{r}')$ and an energy function $F(z)$:

$$G(\mathbf{r}, \mathbf{r}', z) = F(z)\Psi(\mathbf{r})\Psi^*(\mathbf{r}') \quad (7)$$

where $|\Psi(\mathbf{r})|^2$ is equal to the density of charge upon a suitable choice of $F(z)$. First, it follows from Eq. 7, that the conjugate complex of the $F(z)\Psi(\mathbf{r})\Psi^*(\mathbf{r}')$ complies with the same relation as the Green's function, i.e. it is equal to the transposed Green's function:

$$G^*(\mathbf{r}', \mathbf{r}, z^*) = [F(z^*)\Psi(\mathbf{r}')\Psi^*(\mathbf{r})]^* = F(z)\Psi^*(\mathbf{r}')\Psi(\mathbf{r}) = G(\mathbf{r}, \mathbf{r}', z) \quad (8)$$

Taking the diagonal Green's function in the limit of real eigenvalues gives:

$$G^\pm(\mathbf{r}, \mathbf{r}, E) = \Psi(\mathbf{r})\Psi^*(\mathbf{r}) \lim_{\eta \rightarrow +0} F(E \pm i\eta) \quad (9)$$

The imaginary part of the diagonal Green's function, integrated over energy, must be equal to the charge density:

$$\begin{aligned} \rho(\mathbf{r}) &= \mp \frac{1}{\pi} \int_{-\infty}^{+\infty} dE \text{Im} G^\pm(\mathbf{r}, \mathbf{r}, E) \\ &= \mp \frac{1}{\pi} \int_{-\infty}^{+\infty} dE \text{Im} \lim_{\eta \rightarrow +0} F(E \pm i\eta) \Psi(\mathbf{r})\Psi^*(\mathbf{r}) \end{aligned} \quad (10)$$

If $\Psi(\mathbf{r})\Psi^*(\mathbf{r}) = \rho(\mathbf{r})$, the rest on the right side must be unity. This is satisfied if

$$\mp \frac{1}{\pi} \text{Im} \lim_{\eta \rightarrow +0} F(E \pm i\eta) = \delta(E - E_0) \quad (11)$$

Using the fact that

$$\lim_{y \rightarrow +0} \frac{1}{x \pm iy} = \mathbb{P} \left(\frac{1}{x} \right) \mp i\pi\delta(x) \quad (12)$$

gives us the explicit form of $F(z)$:

$$F(z) = \frac{1}{z - E_0} \quad (13)$$

Thus, the Green's function can be written as the product of two local phase correlation functions[12]:

$$G(\mathbf{r}, \mathbf{r}', z) = \frac{\Psi(\mathbf{r})\Psi^*(\mathbf{r}')}{z - E_0} \quad (14)$$

At this stage we have shown that the phase correlation function $\Psi(\mathbf{r})$ is an *exact* representation of the N -electron system, as long as the system can be described by a Green's function Eq. 4. However, it is not yet clear, whether there is a differential equation describing the evolution of $\Psi(\mathbf{r})$. This equation cannot be equal to the standard Kohn-Sham equations, as this would lead to a non-local concept. If we write the Hamiltonian $H(\mathbf{r}, \mathbf{r}')$ as the sum:

$$H(\mathbf{r}, \mathbf{r}') = H(\mathbf{r}) + H(\mathbf{r}') - H_1(\mathbf{r})H_1^*(\mathbf{r}'), \quad (15)$$

and insert into Eq. 6 we get:

$$\begin{aligned} & \frac{\Psi^*(\mathbf{r}') [H(\mathbf{r}) - z] \Psi(\mathbf{r})}{z - E_0} + \frac{\Psi(\mathbf{r}) [H(\mathbf{r}') - z] \Psi^*(\mathbf{r}')}{z - E_0} - \\ & - \frac{[H_1(\mathbf{r})H_1^*(\mathbf{r}') - z] \Psi(\mathbf{r})\Psi^*(\mathbf{r}')}{z - E_0} = -\delta(\mathbf{r} - \mathbf{r}') \end{aligned} \quad (16)$$

It can be seen that the second line contains a product of operators at different locations \mathbf{r} and \mathbf{r}' . This would mean that the phase correlation at a point \mathbf{r} depends on events at point \mathbf{r}' , even though there is no obvious connection. However, since Ψ depends only on \mathbf{r} , this seems unjustified. In addition, the Hohenberg-Kohn theorem proves that if $|\Psi(\mathbf{r})|^2$ is equal to the groundstate density of charge, then an energy eigenvalue E_0 is defined and must be equal to the total energy. Therefore it should be possible to formulate the problem of finding the phase correlation function $\Psi(\mathbf{r})$ in an eigenvalue equation. In this case the many-electron Green's function has only one pole, in contrast to the standard spectral decomposition, where it has N poles.

Here we make the only conjecture in this paper: we assume that the phase correlation function $\Psi(\mathbf{r})$ is described by a suitable modification of a single coordinate Schrödinger equation:

$$-\frac{\hbar^2}{2m}\nabla^2\Psi(\mathbf{r}) + U(\mathbf{r})\Psi(\mathbf{r}) = E_0\Psi(\mathbf{r}) \quad (17)$$

with a local potential $U(\mathbf{r})$. That such a modification is possible and leads to correct results in simple test cases, will be shown in the following. The conjecture is supported by the derivation of an approximate single coordinate Schrödinger equation from the Hartree-Fock model of an N -electron system [13].

If this conjecture is justified, then we have obtained, at this point, a phase correlation function, which includes all phase correlations in the occupied range, it complies with a local equation, its corresponding eigenvalue E_0 is equal to the total energy of the system, and its square gives the electron charge density in the system. This entity looks very much like a descriptor of the physical system

itself. Something, which is otherwise called a many-body wavefunction. As this term might lead to confusion, since the many-body wavefunction is in standard theory described by N local coordinates $(\mathbf{r}_1, \mathbf{r}_2, \mathbf{r}_3, \dots, \mathbf{r}_N)$, we shall call it the *many-electron* wavefunction in the rest of the paper.

An additional note concerning the relation of the framework presented in this paper to density functional theory seems necessary. In particular, since the original derivation of the Hohenberg-Kohn theorem is based on many-body wavefunctions [1]. In this respect we note that the groundstate charge density, once obtained, can be written in any representation. Thus an energy minimum, associated with a density, is enough to describe the physical content of a many-electron system. As long as the energy is a minimum, it is therefore irrelevant, how this minimum was obtained in practice. This is reflected by the most efficient methods in density functional theory, which are based on trial wavefunctions, which do not diagonalize the Hamiltonian. Instead, the off-diagonal elements are minimized with the help of numerical algorithms until they vanish.

2.2 The non-linear Schrödinger equation

So far, we have not considered the modified form of the Hamiltonian $H(\mathbf{r})$. In particular the potential, which in the standard formulation is the potential of single electrons, is not suitable for our purposes. To find a local formulation of the problem, we start with the Schrödinger equation of the many-electron system, written as:

$$-\frac{\hbar^2}{2m}\nabla^2\Psi(\mathbf{r}) + U(\mathbf{r})\Psi(\mathbf{r}) = E\Psi(\mathbf{r}) \quad (18)$$

Here, ∇^2 denotes the Laplacian, $U(\mathbf{r})$ a potential in the system, and E the total energy. Within the context of density functional theory it is generally assumed that the potential U reflects the interaction between the charge of one electron, and the potential of the environment. This entails that the potential is a sum containing the positions of all electrons in the system. While such an approach is possible, it does not reflect the previous findings. If phase correlations and charge are local quantities, then the interactions between electron charge and the potential of all other charges should also be local.

The single coordinate equation 18 must therefore be recast into a relation based on densities, and not integral quantities. This provides the desired equation for the many-electron wavefunction. If $U(\mathbf{r})$ is e.g. the Coulomb potential of an ion with charge Z , then the potential density of electron attraction at a point (\mathbf{r}) is given by:

$$v(\mathbf{r})\rho(\mathbf{r}) = -\frac{1}{4\pi\epsilon_0}\frac{Ze^2\rho(\mathbf{r})}{|\mathbf{r} - \mathbf{R}_{ion}|} \quad v(\mathbf{r}) = -\frac{1}{4\pi\epsilon_0}\frac{Ze^2}{|\mathbf{r} - \mathbf{R}_{ion}|} \quad (19)$$

Similarly, the kinetic energy term and the total energy will change into kinetic energy density and total energy density. The variables in the local equation will

be changed into:

$$\frac{\hbar^2}{2m} \Rightarrow 2f \quad U(\mathbf{r}) \Rightarrow v(\mathbf{r})\rho(\mathbf{r}) \quad E \Rightarrow \epsilon \quad (20)$$

f is a system parameter, related to the volume of the system, which shall be analysed in detail further down. $v(\mathbf{r})$ is the external potential. ϵ is the energy density. The equation then reads:

$$-2f\nabla^2\Psi(\mathbf{r}) + v(\mathbf{r})\rho(\mathbf{r})\Psi(\mathbf{r}) = \epsilon\Psi(\mathbf{r}) \quad (21)$$

2.2.1 External potential

The interaction between electrons and ions in a groundstate many-body problem is exclusively described by Coulomb interactions. If $\Psi(\mathbf{r})$, as shown in previous sections, uniquely describes the problem, then the same should hold for the modified Schrödinger equation. Exchange correlation potentials, as in density functional theory, would enter the description only at the level of single electron states. Since $\Psi(\mathbf{r})$ describes the total system, and not single electron state, they will not enter the present framework. However, Coulomb interactions will be modified, if one considers magnetic systems. In this case the potential $v(\mathbf{r})$ will depend on the spin-state of electron charge. At present, we do not consider this case. The potential $v(\mathbf{r})$ then is the Coulomb interaction potential due to electrons and ions,

$$v(\mathbf{r}) = \frac{e^2}{4\pi\epsilon_0} \left[\int d^3r' \frac{\rho(\mathbf{r}')}{|\mathbf{r} - \mathbf{r}'|} - \sum_{i=1}^M \frac{Z_i}{|\mathbf{r} - \mathbf{R}_i|} \right] \quad (22)$$

2.2.2 Charge density

The density of charge $\rho(\mathbf{r})$ is the square of the many-electron wavefunction, or:

$$\rho(\mathbf{r}) = \Psi^*(\mathbf{r})\Psi(\mathbf{r}) \quad (23)$$

Writing an equivalent equation for the complex conjugate function $\Psi^*(\mathbf{r})$, we get:

$$-2f\nabla^2\Psi^*(\mathbf{r}) + v(\mathbf{r})\rho(\mathbf{r})\Psi^*(\mathbf{r}) = \epsilon\Psi^*(\mathbf{r}) \quad (24)$$

Multiplying the first of these equations by $\Psi^*(\mathbf{r})$, and the second by $\Psi(\mathbf{r})$, and adding the equations, we end up with:

$$-f [\Psi^*(\mathbf{r})\nabla^2\Psi(\mathbf{r}) + \Psi(\mathbf{r})\nabla^2\Psi^*(\mathbf{r})] + v(\mathbf{r})\rho(\mathbf{r})\rho(\mathbf{r}) = \epsilon\rho(\mathbf{r}) \quad (25)$$

The Laplacian acting on the density is given by:

$$\begin{aligned} \nabla^2 [\Psi(\mathbf{r})\Psi^*(\mathbf{r})] &= [\Psi^*(\mathbf{r})\nabla^2\Psi(\mathbf{r}) + \Psi(\mathbf{r})\nabla^2\Psi^*(\mathbf{r})] + \\ &+ 2 [\nabla\Psi(\mathbf{r})] [\nabla\Psi^*(\mathbf{r})] \end{aligned} \quad (26)$$

The second term on the right contains the essential phase correlations of the many-electron wavefunction. We symbolize it by $\Pi[\Psi]$ to denote that it contains

the many-electron phase correlations. In principle there seems no straightforward method to describe it in terms of charge densities alone: as the many-electron system has to be phase coherent, the density of charge alone provides insufficient information. If this were not the case, then a formulation based on density alone would be sufficient to describe the physical content of a many-electron system. From this viewpoint, the essential finding of density functional theory is not only the uniqueness of the charge distribution, but also of the groundstate energy. This energy, in turn, can only be determined by constructing a phase coherent system. Thus the density of charge will be described by:

$$\begin{aligned} [-f\nabla^2 + v(\mathbf{r})\rho(\mathbf{r})] \rho(\mathbf{r}) + f\Pi[\Psi] &= \epsilon\rho(\mathbf{r}) \\ \Pi[\Psi] &= 2[\nabla\Psi(\mathbf{r})][\nabla\Psi^*(\mathbf{r})] \end{aligned} \quad (27)$$

However, the non-linear equation describes the many-electron wavefunction, provided the potential and groundstate charge density are known. It is therefore not strictly necessary to find a formulation based on density alone, as long as the nonlinear equation leads to correct many-electron wavefunctions. The derivation thus provides a set of three equations, defining the groundstate of a system:

$$\begin{aligned} [-2f\nabla^2 + v(\mathbf{r})\rho(\mathbf{r})] \Psi(\mathbf{r}) &= \epsilon\Psi(\mathbf{r}) \\ [-f\nabla^2 + v(\mathbf{r})\rho(\mathbf{r})] \rho(\mathbf{r}) + f\Pi[\Psi] &= \epsilon\rho(\mathbf{r}) \\ \rho(\mathbf{r}) &= \Psi(\mathbf{r})\Psi^*(\mathbf{r}) \end{aligned} \quad (28)$$

Note that this set of equations applies to the many-electron density of charge without any reference to single Kohn-Sham states. It describes the physical system by four variables: the density of charge $\rho(\mathbf{r})$, the external potential $v(\mathbf{r})$, which will also depend on the density, the energy density ϵ , and the many-electron wavefunction $\Psi(\mathbf{r})$. The equations lead to a direct method of calculating the groundstate charge density by solving the nonlinear Schrödinger equation and minimizing the energy density ϵ of the system. The self-consistent procedure, elaborated in the following section, will be

- make an initial guess for the density ρ_0 ,
- construct the potential v_0 ,
- solve the nonlinear Schrödinger equation for Ψ , and
- construct a new charge density $\rho_1 = \Psi^*\Psi$.

The cycle is repeated until input and output charge densities are equal. The problem of finding the groundstate energy density can be formulated as the following minimization problem:

$$\epsilon = \left\{ \frac{\int d^3\mathbf{r} \left([-f\nabla^2 + v(\mathbf{r})\rho(\mathbf{r})] \rho(\mathbf{r}) + f\Pi[\Psi(\mathbf{r})] \right)}{\int d^3\mathbf{r} \rho(\mathbf{r})} \right\}_{Min} \quad (29)$$

Note that also in this case the problem cannot be formulated as a minimization problem of charge density alone. This is a consequence of basing the whole derivation on the many-electron problem and ensuring the phase coherence throughout the system.

2.3 Physical implications

From a dimensional point of view it is interesting to analyse the meaning of the system constant f . Its dimension is that of a force:

$$[f\nabla^2] = \left[\frac{E}{L^3} \right] \quad [f] = \left[\frac{E}{L^3} L^2 \right] = \left[\frac{E}{L} \right] = N(SI) \quad (30)$$

Apart from the universal constants \hbar and m the system constant f only depends on the volume. In this respect, it is beyond the well known Thomas-Fermi model, where the kinetic energy density is system independent. The second difference is that phase correlations are included in the picture, by solving the non-linear Schrödinger equation. The differences are crucial. As shown in the following sections, the model recaptures the density oscillations at metal surfaces, contrary to the Thomas-Fermi model. That the kinetic energy density *cannot* be system independent, is in line with observations in quantum mechanics that the energy of a system comprising e.g. a single electron is inverse proportional to the enclosing volume. It seems therefore that the action of an external potential on the density of charge can be seen as a force acting on the wavevector, or the spatial distribution of the density. The reason for this force is that energy at a given point of the system has to be conserved. The reason that it acts on the curvature rather than the amplitude is the relation between curvature or wavevector and kinetic energy, predicted by Louis de Broglie, and experimentally confirmed by Davisson and Germer [14, 15].

Since ϵ was defined as the total energy divided by the volume the equation has an additional physical content. A solution of the equation with constant ϵ means that the energy density does not vary from one point of the system to another. From the viewpoint of thermodynamics, this is also the condition of a system in equilibrium. One could thus say that the specific form of the Schrödinger equation has one very specific physical meaning: it provides the solution of distributing electron charge in an external potential in such a way, that the energy density is constant. It explains, why the mathematical form of the equation is different from e.g. a differential equation in classical electrodynamics. There, the boundary conditions usually lead to a selection of amplitudes and frequencies in a system. Here, the frequencies need to be modified at every single point in order to achieve constant energy density values. In principle, this is still a wave-dynamical problem, but a problem modified by the ability of electrons to interact with external potentials and with each other. This formulation of the many-electron problem also explains, why wave mechanics, based on the Schrödinger equation, *appears* to be non-local [16]: since the main condition implicitly contained in the equation is the condition of thermal equilibrium, one cannot separate one part of the system from any other part, without contradicting the assumption that the system as a whole will equilibrate. Thus, wave mechanics is in fact a local theory, like every other theory known in physics, but it is applied to systems which are assumed to be connected throughout. This can clearly be seen in the mathematical form of Eqs. 28: all variables of the system, $v(\mathbf{r}), \rho(\mathbf{r})$, and ϵ are local scalars, defined at a specific point of the

system. These local variables cannot, however, be arbitrarily chosen, since ϵ *must* be a constant and f *must* relate to the volume of the system.

One might object, at this point, that the problem is now vastly more complicated. After all, the eigenvalue problem is now non-linear, and it is generally impossible to compute solutions of non-linear differential equations in full generality. Here, we remember the main result of the Hohenberg-Kohn theorem: the groundstate charge density is the charge density, which minimizes the total energy and thus the energy density ϵ . This shall provide, as will be seen, a way to compute the exact solution starting from an initial guess for the charge density $\rho(\mathbf{r})$, by solving a linear eigenvalue equation and adjusting the charge density from one iteration to the next. In principle, it is a very similar method to the one used today in standard DFT codes, but for two decisive advantages:

1. The charge density is computed directly without any reference to single-particle Schrödinger equations.
2. The charge density computed is the many-electron charge density and it is therefore completely independent of exchange-correlation functionals and density approximations.

2.4 Possible objections

From a pragmatic point of view, the approach seems not too different to the standard approach, apart from the fact that the non-local density-correlations in the potential have been replaced by the charge density itself. However, there is a number of issues, related to non-linear concepts, which deserve a closer look.

- If the Hohenberg-Kohn theorem is correct, then the groundstate charge density is unique. Here, we have a non-linear potential, and the groundstate is therefore potentially not unique.

There are two possible answers. The first is the current state of DFT itself. After all, exchange correlation functionals *include* the density and its derivatives. The effective potential in today's DFT simulations is therefore also non-linear. This, it seems, does not invalidate the results of calculations. The second is based on recent research (in Mathematics) on the behavior of non-linear Schrödinger equations, related to weak coupling in a many-electron systems [13]: in this case the equations still yield physically acceptable solutions, even though the existence of a solution depends on reasonable physical conditions.

- The Thomas-Fermi model also attempts to calculate charge densities from a non-linear potential and a kinetic energy density. The same seems to be tried here. But we know that this model fails even to explain chemical bonding.

The answer to this question lies in the treatment of the kinetic energy term, and the use of the nonlinear Schrödinger equation to determine many-electron charge densities. Within the Thomas-Fermi model, the prefactor of the kinetic

energy functional is a constant. This means, that it does not depend on the system, but is universally the same. Physically speaking, this cannot be correct. Because an electron in a very large negative potential *must* experience different kinetic effects than an electron in a comparatively small negative potential. In the present model the kinetic energy density is inversely proportional to the volume, and contains a term which is directly related to the many-electron phase correlations. It will be seen in the simulation of metal surfaces, that this leads to the correct behavior of electrons at a boundary.

- I do not see spin-statistics involved in this approach. In standard DFT this is part of the exchange-correlation functionals. Where is it in this formulation?

Here, one has to note that spin-statistics are also not involved in the formulation of the non-magnetic many-electron Schrödinger equation. They only arise at the level, where single electrons are thought of as individual entities. A many-electron wavefunction in a many-electron Schrödinger equation is a unique scalar function of location and spin. In a non-magnetic formulation only of location. So far, we have not included spin in the framework. This must be done in field mediated manner and will be the topic of future work.

- Non-linearity is nothing new. It is already present in the standard techniques, since self-consistency cycles are essentially non-linear. The non-linearity lies therefore in the variational principle, but not in the fundamental equations.

While we do not dispute that the variation and the ensuing self-consistency cycles are non-linear, the fundamental equations, the Kohn-Sham equations, are still linear. If this were not the case, then the groundstate of a system *could not* be described as a superposition of N single electron states. While this, we think, is correct for a mean-field theory, it is not suitable within a many-electron framework. In this sense the described approach extends the non-linearity to the fundamental equations themselves, with the effect, that superpositions are no longer possible. The groundstate calculated with this approach cannot be decomposed into single-electron states, or only, if one uses an approximation.

Before sketching the solution of the eigenvalue problem, let us consider some limiting cases, where one can show that the linear Schrödinger equation is in fact the zero order approximation of the general problem.

2.5 Zero order approximations

The main areas, where the Schrödinger equation is used today, are the theory of atoms, and solid state theory. In solid state theory the most frequently employed DFT codes use periodic boundary conditions and are generally applied to systems with translational symmetry. In quantum chemistry, DFT methods usually focus on atomic orbitals and their representation by suitable basis sets.

Let us consider initially an atomic system, where the density of charge can be closely mimicked by an exponential function. Thus, with radial symmetry:

$$\rho(r) = \rho_0 \exp(-\kappa r) \quad (31)$$

The expansion of the exponential function gives:

$$\rho(r) = \rho_0 \left(1 - \frac{\kappa r}{1!} + \frac{(\kappa r)^2}{2!} - \frac{(\kappa r)^3}{3!} + \dots \right) \quad (32)$$

The zero order approximation assumes that $\rho(r) = \rho_0 = \text{constant}$. Inserting ρ_0 into Eq. 21, and multiplying by the volume V , we get:

$$-2fV\nabla^2\Psi(\mathbf{r}) + v_{nl}(\mathbf{r})\rho_0V\Psi(\mathbf{r}) = E\Psi(\mathbf{r}) \quad (33)$$

Setting $2fV = \hbar^2/2m$ we arrive at the conventional Schrödinger equation, e.g. for the hydrogen atom:

$$\left[-\frac{\hbar^2}{2m}\nabla^2 + U(\mathbf{r}) \right] \Psi(\mathbf{r}) = E\Psi(\mathbf{r}) \quad (34)$$

In solid state physics, systems are generally periodic. The density of charge in this case will be a periodic function. For the sake of demonstration we use a cosine, but the same argument applies to a sine or an imaginary exponent. Say, we can write the density of charge as:

$$\begin{aligned} \rho(\mathbf{r}) &= \alpha(1 + \beta \cos(\mathbf{k}\mathbf{r})) = \alpha + \\ &+ \alpha \cdot \beta \left(1 - \frac{(\mathbf{k}\mathbf{r})^2}{2!} + \frac{(\mathbf{k}\mathbf{r})^4}{4!} - \frac{(\mathbf{k}\mathbf{r})^6}{6!} + \dots \right) \end{aligned} \quad (35)$$

where \mathbf{k} is a vector in reciprocal space, and $\beta < 1$. We set $\alpha + \alpha \cdot \beta = \rho_0$. Then the zero order approximation for the non-linear eigenvalue problem will read (we have again multiplied by the volume V):

$$-2fV\nabla^2\Psi(\mathbf{r}) + v_{nl}(\mathbf{r})\rho_0V\Psi(\mathbf{r}) = E\Psi(\mathbf{r}), \quad (36)$$

and it will again lead to the conventional Schrödinger equation if we set $2fV = \hbar^2/2m$:

$$\left[-\frac{\hbar^2}{2m}\nabla^2 + U(\mathbf{r}) \right] \Psi(\mathbf{r}) = E\Psi(\mathbf{r}) \quad (37)$$

We are well aware that these examples do not constitute a proof that the non-linear eigenvalue problem is exactly equivalent to the Schrödinger equation. In fact, if this were the case, then the whole formulation might be considered redundant, since it is only a different way of stating what is already known.

2.6 Removing the paradoxes from quantum mechanics

The new framework removes two of the fundamental problems in quantum mechanics, which have been the subject of debate almost from the beginning of modern physics. It is probably not exaggerated to say that the research done on quantum paradoxes has, over the years, produced a volume of work comparable to the volume of work in standard developments.

1. The Schrödinger cat paradox [17]. In the standard formulation the cat is either dead, or alive, but its state can only be determined by a measurement. There is, fundamentally, no objective way of deciding before a measurement.
2. The Einstein-Podolsky-Rosen paradox [18]. In this case a quantum mechanical system is thought to be split into two subsystems which increase their distance with the velocity of light. After some time two separate measurements are performed on either subsystem, and according to the standard formulation, the measurement on one subsystem should determine the measurement on the second one, even though no physical interaction is known which exceeds the speed of light.

Both paradoxes rest on one fundamental feature of systems in standard quantum mechanics: the first, on the possibility of superimposing separate solutions of the Schrödinger equation to describe the state of a system; the second, on the very same feature with a slight modification concerning the times of measurement and the critical distance between the subsystems. The resolution of the paradoxes, within this new framework, is the easiest possible answer: the cat is dead, or it is alive, independent from any measurement, because there exists at any given moment only one unique solution to the fundamental equations. This is a consequence of the non-linearity of the general framework, as already pointed out. The same applies to the second paradox, with the slight modification, that performing a measurement on one subsystem changes the state of this subsystem. While in the standard framework, this has an effect on the second subsystem, since the state of the overall system is described by a superposition, it does not affect the second subsystem in the present framework, since the fundamental principle of equilibration would be violated. The second subsystem *cannot* equilibrate with the first one, *because* it cannot interact.

From a physical point of view, this resolution of the paradoxes seems actually more in keeping with a materialistic mindset. Physicists of a classical disposition have been arguing against the consequences of the mathematical framework, and in particular the feature of superposition, for almost a century. Here, we adopt the view that this consequence hinges on the linearity of the Schrödinger equation, and that this linearity is actually a feature enforced by the approximations used.

3 Iterative solution of the non-linear eigenvalue problem

While some eighty years ago the non-linear problem would have been unsolvable, this has changed significantly over the last fifty years due to the existence of powerful computers. In this respect, theory is not much different from experiments: a change in the equipment usually leads to a different focus in research, as phenomena, which were previously out of range, can now be analysed in a scientific manner.

In particular the advent of DFT and the continuous improvement of computing algorithms applied to solid state physics have created an environment in theory, where the inability to solve equations analytically is no hindrance. Two of the main problems, needed to solve the non-linear problem, are already incorporated in standard DFT codes: (i) The problem of finding the charge density ρ_{i+1} after a given iteration i . This is done by elaborate mixing schemes, which are constructed to speed up the convergency process. (ii) The problem of finding the minimum energy density. This problem is not different from the problem of finding it in standard DFT convergency cycles, where one aims at processing with the calculation along a hyper-surface, which will lead to a minimum. In fact, if the charge density is a unique functional for a given system, then the convergence criterium can be reformulated in terms of the difference of charge in two subsequent iteration cycles: if this difference is zero, then the charge density is the true groundstate charge density. Thus the problem of finding the solution of the non-linear eigenvalue problem and the groundstate charge density from:

$$[-2f\nabla^2 + v(\mathbf{r})\rho(\mathbf{r})] \Psi(\mathbf{r}) = \epsilon\Psi(\mathbf{r}) \quad (38)$$

can be broken down in a number of discrete steps. Let us consider a general case; a system with a number M of ions, at the positions \mathbf{R}_i of our coordinate system. The number of electrons N shall be:

$$N = \int d^3\mathbf{r} \Psi^*(\mathbf{r})\Psi(\mathbf{r}) = \int d^3\mathbf{r} \rho(\mathbf{r}) = \sum_{i=1}^M Z_i \quad (39)$$

if the system is neutral and the ionic charge of atom i is given by Z_i . If we neglect for the time being magnetic systems, then the potential $v(\mathbf{r})$ is the sum of ionic and electronic contributions; it can be written as (we use atomic units in the rest of the paper):

$$v(\mathbf{r}) = - \sum_{i=1}^M \frac{Z_i}{|\mathbf{r} - \mathbf{R}_i|} + \int d^3\mathbf{r}' \frac{\rho(\mathbf{r}')}{|\mathbf{r} - \mathbf{r}'|} \quad (40)$$

Then the potential part of the eigenvalue equation is described by (we follow the convention in DFT and write the product of external potential and charge

density as the effective potential $v_{eff}(\mathbf{r})$):

$$v_{eff}(\mathbf{r}) = v(\mathbf{r})\rho(\mathbf{r}) = - \sum_{i=1}^M \frac{\rho(\mathbf{r})Z_i}{|\mathbf{r} - \mathbf{R}_i|} + \int d^3\mathbf{r}' \frac{\rho(\mathbf{r})\rho(\mathbf{r}')}{|\mathbf{r} - \mathbf{r}'|} \quad (41)$$

The eigenvalue problem then has the form:

$$[-2f\nabla^2 + v_{eff}(\mathbf{r})] \Psi(\mathbf{r}) = \epsilon\Psi(\mathbf{r}) \quad (42)$$

A minimization process proceeds from one charge density to the next without the calculation of Kohn-Sham eigenstates. One may wonder that the parameter f , related to the kinetic energy density, still contains the volume. This is a consequence of the rigorous application of the energy principle, not only for the system as a whole, but for every single point. If the density of charge is increased, then the potential energy will also increase. This, in turn means that the kinetic energy density will be lower. Given a number of electrons in the system, all energy components depend on the volume. The volume must therefore also show up in the kinetic energy component.

3.1 Initial charge density

It is customary in DFT simulations to start a self-consistency cycle with an initial guess about the charge density distribution. In principle, this guess could involve any arbitrary choice, as long as the total number of electrons in the system is equal to N . However, most codes employ a superposition of atomic charges. As the previous section and the zero order approximation of the non-linear problem show, this is a suitable choice for the present problem. Since the charge density will ultimately be computed self-consistently, we may employ this approximation also for our initial charge distribution, setting $\rho_0(\mathbf{r})$ to:

$$\rho_0(\mathbf{r}) = \sum_{i=1}^M \sum_{\alpha=1}^{Z_i} \rho_{\alpha,i}(\mathbf{r} - \mathbf{R}_i) \quad (43)$$

where α indicates the atomic orbitals of a given atom at the position \mathbf{R}_i . From this initial charge density the potential $v_{eff,0}(\mathbf{r})$ is computed with:

$$v_{eff,0}(\mathbf{r}) = - \sum_{i=1}^M \frac{\rho_0(\mathbf{r})Z_i}{|\mathbf{r} - \mathbf{R}_i|} + \int d^3\mathbf{r}' \frac{\rho_0(\mathbf{r})\rho_0(\mathbf{r}')}{|\mathbf{r} - \mathbf{r}'|} \quad (44)$$

3.2 Self consistency cycle

The initial potential is the input for the first iterative cycle to solve the ensuing *linear* density equation:

$$[-2f\nabla^2 + v_{eff,0}(\mathbf{r})] \Psi(\mathbf{r}) = \epsilon\Psi(\mathbf{r}) \quad (45)$$

The problem is a standard problem in DFT, and a large number of algorithms exists for its solution. Note that it is only necessary to calculate the lowest eigenstate, defined by ϵ_1 , and the corresponding real eigenvector $\rho_1(\mathbf{r})$. This is in marked contrast with today's methods, where an N electron system has to be solved for N eigenvalues and eigenvectors. This means, that the size of the problem depends only on the volume of the system. If we consider that the volume usually scales linearly with the number of atoms, then the ensuing numerical problem is also of the same size. Apart from the simplification of not having to solve the Schrödinger equation for single Kohn-Sham states the new method scales also much better than usual codes, which scale quadratically or cubic with N . It is a true order- N method, or provides the optimum scaling with the size of the system. Today, order- N methods are based on a clever use of density matrices (see e.g [4]), or they use atomic orbitals [19], which makes them unsuitable for metallic systems. The suggested method has no limitation in this respect. Once the many-electron wavefunction is known, the charge density is given by:

$$\rho_1(\mathbf{r}) = \Psi_0^*(\mathbf{r})\Psi_0(\mathbf{r}) \quad (46)$$

The density $\rho_1(\mathbf{r})$ is used to construct a new potential, $v_{eff,1}(\mathbf{r})$, by mixing the input density $\rho_0(\mathbf{r})$ and the output density $\rho_1(\mathbf{r})$ with the help of a suitable mixing algorithm, so that:

$$\rho_1(\mathbf{r}) = \mathcal{M}[\rho_0(\mathbf{r}), \rho_1(\mathbf{r})] \quad (47)$$

Again, this is standard procedure in today's DFT codes and a large number of mixing schemes (see e.g. [20, 21, 22]) exists to guarantee numerical stability in the self-consistency cycle. The new potential $v_{eff,1}(\mathbf{r})$ is then:

$$v_{eff,1}(\mathbf{r}) = - \sum_{i=1}^M \frac{\rho_1(\mathbf{r})Z_i}{|\mathbf{r} - \mathbf{R}_i|} + \int d^3\mathbf{r}' \frac{\rho_1(\mathbf{r})\rho_1(\mathbf{r}')}{|\mathbf{r} - \mathbf{r}'|} \quad (48)$$

And the second iteration cycle consists again of solving a linear eigenvalue problem described by:

$$[-2f\nabla^2 + v_{eff,1}(\mathbf{r})] \Psi(\mathbf{r}) = \epsilon\Psi(\mathbf{r}) \quad (49)$$

A solution of the problem leads to energy eigenvalue ϵ_2 and eigenvector $\Psi_2(\mathbf{r})$, which are used as an input for the new effective potential $v_{eff,2}(\mathbf{r})$. The iteration is repeated until convergency, usually defined either by the change of eigenvalues or the change of charge density, is achieved.

3.3 Calculating the value of physical variables

Once the groundstate charge density $\rho_g(\mathbf{r})$ has been computed the many-electron wavefunction can be determined by solving the eigenvalue problem:

$$[-2f\nabla^2 + v_g(\mathbf{r})\rho_g(\mathbf{r})] \Psi(\mathbf{r}) = \epsilon\Psi(\mathbf{r}) \quad (50)$$

The many-electron wavefunction may provide a direct way in the future to compute all physical quantities of interest. Since the many-electron wavefunction is the solution of the non-linear Hamiltonian, the density matrix:

$$n(\mathbf{r}, \mathbf{r}') = \Psi(\mathbf{r})\Psi^*(\mathbf{r}') \quad (51)$$

can be used to calculate any physical quantity A of interest via:

$$\langle A \rangle = Tr [A\Psi(\mathbf{r})\Psi^*(\mathbf{r}')] = \int d^3\mathbf{r} A\rho(\mathbf{r}) \quad (52)$$

However, the physical quantities like kinetic energy and potential energy have been modified to obtain the general formulation. Similarly, other quantities in the Schrödinger equation, e.g. momenta, or electric field operators, will have to be adapted to the non-linear formulation.

An alternative solution to the problem which allows to make use of the vast body of theory developed, will be to use only the many-electron groundstate charge density $\rho_g(\mathbf{r})$, and to construct the effective potential in the standard way by:

$$v_{eff,dft}(\mathbf{r}) = v[\rho_g(\mathbf{r})] \quad (53)$$

This effective potential then allows to construct single particle solutions in the standard manner:

$$\left\{ -\frac{1}{2}\nabla^2 + v[\rho_g(\mathbf{r})] \right\} \psi_i(\mathbf{r}) = \epsilon_i \psi_i(\mathbf{r}) \quad (54)$$

These solutions can be used within the standard framework, considering that the groundstate charge density completely determines the physical properties of the system. The forces on ions in a system can be calculated in the usual manner. Since the Hamiltonian of the non-linear formulation is still hermitian, the Hellman-Feynman theorem still applies [23]:

$$\mathbf{F}_i = -\frac{\partial E}{\partial \mathbf{R}_i} = -\int d^3\mathbf{r} \rho(\mathbf{r}) \frac{\partial v(\mathbf{r})\rho(\mathbf{r})}{\partial \mathbf{R}_i} \quad (55)$$

From this relation the forces on atomic nuclei can be calculated in the standard manner. These forces can then be used to optimize the geometry of the system.

3.4 Summary

We have shown in this section that the non-linear formulation of density functional theory allows to perform standard iteration procedures as used for at least three decades. It was pointed out that the main advantages of the new approach are:

1. The iterations lead to the true many-electron charge density.
2. The complexity of the calculation scales linearly with the number of atoms

Metal	Type	a [a.u.]	V [a.u. ³]	e/cell	r_s	Φ [eV]
Cs	bcc	11.6	1560.9	2	5.74	1.81
Li	bcc	6.63	291.4	2	3.26	2.38
Cu	fcc	6.83	318.8	44	1.20	4.40
W	bcc	5.98	214.0	12	1.62	4.50

Table 1: Lattice parameters, Wigner-Seitz radii of electrons, and workfunction of typical metals. The experimental workfunctions were taken from [24], the lattice parameters from [25]

4 Numerical tests

Lang and Kohn showed in the early Seventies [26, 27] that the electron charge at the surface of a metal oscillates as it approaches the surface dipole. While standard DFT is able to capture this behavior, the Friedel-oscillations, the Thomas-Fermi method fails quite dramatically. It seems therefore an ideal test case for non-linear DFT. The typical density of metals can be inferred from the lattice type, the lattice constant, and the number of valence electrons, assuming that the core covers only a small region of the unit cell. The Wigner-Seitz radii of typical metals, as well as their experimental workfunctions, are given in Table 1.

4.1 Setup

We performed self-consistent simulations of the groundstate charge density for a metallic system, varying the density of the positive background in the jellium calculation from $r_s = 3$ to $r_s = 1.5$ a.u. The metal was modeled by a slab of $30(r_s=1.5-2.0$ a.u.) to 40 a.u.($r_s = 2.5-3.0$ a.u.) thickness, corresponding to more than 15 layers of the metal. In standard DFT simulations this is sufficient to guarantee bulk properties in the center of the slab. In all calculations the film was embedded in two vacua, the vacuum range was 15-20 Bohr radii. This seems sufficient to mimic the surface potential barrier, it should also allow to estimate, whether the density decays exponentially into the vacuum range, as found in standard DFT simulations [26, 27], or inversely proportional with the distance from the jellium edge, as required by the asymptotic decay due to image potentials. The non-linear equation of the problem has the following form:

$$\left[-\frac{1}{2} \frac{d^2}{dz^2} + v_{nl}(z) \right] \Psi(z) = E\Psi(z) \quad (56)$$

Here, the eigenvalue E is the energy value of the many-electron electron charge. With a suitably chosen non-linear potential it will be equal to the eigenvalue of the many-electron Schrödinger equation. The dipole potential of the surface can be calculated in the standard way by integrating the contributions from a

point deep inside the jellium into the vacuum region[26, 27]:

$$v_{el}(z) = -4\pi \int_z^\infty dz' \int_{z'}^\infty dz'' [\rho(z'') - \rho_+(z'')], \quad (57)$$

and by using the boundary condition $v_{el}(z \rightarrow \infty) = 0$. The nonlinear potential was obtained by multiplying the dipole potential with $V_{ws}\rho(z)$, where V_{ws} is the Wigner-Seitz volume:

$$v_{nl}(z) = v_{el}(z)V_{ws}\rho(z) \quad V_{ws} = \frac{4\pi}{3}r_s^3 \quad (58)$$

The initial surface dipole was mimicked by a Fermi distribution function at both jellium edges. The initial density in the vacuum at a distance of 20a.u. was below 10^{-17} in units of the jellium density. The initial nonlinear potential is nearly equal to the electrostatic potential inside the slab, the only significant differences occur at the jellium edges (see Fig. 1). Conveniently, the nonlinear potential also has the same dimensions as the electrostatic potential. It starts deviating only, once the electron charge density in the initial setup differs substantially from the positive background.

4.2 Iterations

The nonlinear equation has been solved by numerical integration. We employed the Numerov integration scheme [28]. The value of Ψ_{n+1} on an equally spaced z-grid is the convolution of the preceding Ψ -values and the second derivative of the equations, according to:

$$\Psi_{n+1} = \frac{2\Psi_n - \Psi_{n-1} + \frac{h^2}{12}(U_{n+1} + 10F_n + F_{n-1})}{1 + \frac{h^2V_{n+1}}{12}} \quad (59)$$

The precision of the result in one step is of the order h^5 , which renders the method quite accurate for one dimensional applications. h is the stepsize in the integration, the derivatives F_n are given by:

$$F_n = 2(v_{nl,n} - E)\Psi_n \quad (60)$$

In case of the non-linear equation U_n will be zero at every gridpoint, while V_n is equal to $2(v_{nl,n} - E)$. The integration is performed twice: once starting from the left, integrating to the right, and once starting from the right and integrating left. The two functions are matched at $z = 0$. The parameter E , the eigenvalue of the system, determines whether they can actually be matched. The standard procedure in this case is to compute the derivatives of the two functions, Ψ_{left} and Ψ_{right} and to change the eigenvalue E until the two functions match. Numerical convergency with a simple linear mixing scheme required a very high number of gridpoints (8000 gridpoints over a length of 60-80a.u.) and very low

mixing parameters (0.001 to 0.002) in the simulation. The difference between input and output charge density is given by the integral:

$$N_d = \frac{1}{N} \int_{-\infty}^{+\infty} dz |\rho_{in}(z) - \rho_{out}(z)| \quad (61)$$

The charge density in the iterations was converged to a value of 0.01, which seemed sufficiently precise. The eigenvalue at this level of convergency is precise to about 1meV. The difference between input and output charge density in the iterations decreases exponentially, as shown in Fig. 2.

4.3 Density oscillations

In the simulations we find, in every case, an oscillation of the charge density at the jellium edge. The wavelength of the oscillation depends on the jellium density. Contrary to Lang and Kohn [26, 27] we do not find that the oscillations are damped for values of $r_s < 2.0$ a.u. The results of the simulations are shown in Fig. 3. We find the same increase of electron density at the jellium edge for every density value. The surplus charge is about 8% compared to the bulk value. The result suggests that within the non-linear framework a gradual removal of the peak and an approach of the Thomas-Fermi result in the limit of $r_s \rightarrow 2$ [26] does not occur. The standard DFT result for a uniform positive background cannot be extended beyond $r_s=3$, as Lang and Kohn showed in their calculations [26, 27]. This feature of the jellium model corresponds to a failure to account for the experimental surface energies in this range. At present, we have not yet developed a method to calculate surface energies from the many-electron charge densities alone. However, it seems quite possible that results remain reasonable also in this range, considering that the surface dipole seems independent of the background charge. Analyzing the details of the density oscillations into the bulk we find a shortening of the wavelength, as the density increases. This is mainly due to changes in the non-linear potential: as the potential becomes more negative, the eigenvalues do not keep up. The positive energy difference between the energy of the electron charge and the potential increases in this case, which leads to shorter wavelengths (see next sections).

4.4 Potentials and eigenvalues

The peak of the charge density at the jellium edge corresponds to a trough in the attractive potential. Compared to the initial potentials (see Fig. 2) the main changes are the deepening of the dip at the barrier and the potential oscillations decaying into the bulk (see Fig. 4). Analyzing the actual process it has to be remembered that the many-electron wavefunction will be in phase throughout the film. As the two partial waves are matched at the center of the film, the actual wavelength is not completely arbitrary but reflects also the boundary conditions. From a physical point of view this is a somewhat unrealistic setup, because the waves will be reflected at the core of bulk atoms. The ensuing

r_s [a.u.]	Eigenvalue [htr]	Φ [eV]	Metal	Φ_{exp} [eV]
3.0	-0.055	1.51	Li	2.38
2.5	-0.073	1.98	Mg	3.64
2.0	-0.102	2.80	Al	4.25
1.5	-0.160	4.35	W	4.50

Table 2: Eigenvalues and workfunctions for different densities. The workfunctions are in the range of 1.5 to 4.35eV, corresponding approximately to the range observed in experiments. Experimental values were taken from [24]. The deviation in the low density regime could be due to the neglect of the core region (see the text).

multiple scattering effects should change the distribution of maxima and minima in a way not reproducible in a one-dimensional model. However, it is quite clear from the results that the many-electron wavefunction will have to be in-phase over a lengthscale of a few nanometer. The coherence can only be broken by electron-phonon interactions in a thermally activated environment. We would therefore conclude that long range effects are a necessary consequence of the present model.

The eigenvalues obtained in the simulations are given in Table 2. They agree very well with experimental data, considering that the model is relatively simple. The only deviations are observed in the low density range $r_s > 3.0$. This could be due either to neglecting the core volume in the calculation of the Wigner-Seitz radius, or to the fact that electron charge in a low density environment will experience the point-like and regular arrangement of the ionic cores much stronger than in a high density environment. In the first case, the actual Wigner-Seitz radius is smaller than the assumed value, in the second case the jellium model is no longer suitable. In experiments the measured values are in the range of 2.0 to 5.0eV. This corresponds to a WS radius in the range of 2.5 to 1.3a.u. Comparing our results for the workfunction with full potential DFT simulations [29], we note that the agreement with experiments for standard transition metals is improved. While in DFT simulations of $5d$ metals the typical workfunctions are well above 5eV, in case of tungsten even above 6eV, they are still in the range of 4-5eV in the present model. We may conclude that the simulations reproduce the experimental values reasonably well, and that the problems occurring in jellium simulations of high density could be due to standard density functional theory itself. Physically speaking, one would expect that a high density of electron charge makes a continuous model more applicable than a low density environment. In standard DFT jellium simulations, one observes exactly the opposite trend [26, 27].

4.5 Vacuum decay

Another reason for obtaining lower workfunctions than in standard DFT could be the vacuum decay of electron density. The value for $r_s=3.0$ at a distance of 20a.u. from the surface in the fully converged system is about 10^{-7} e/a.u.³. This is ten orders of magnitude higher than at the beginning of the self consistency loop. It is also three to four orders of magnitude higher than in standard DFT simulations. A logarithmic plot of the vacuum density reveals quite clearly, that the density *does not* decay exponentially in the long distance limit. Logarithmic plots of all systems are shown in Fig. 5. The curves deviate from an exponential characteristic. The inset shows a fit of the density to two graphs: (i) An exponential with the decay constant equal to $\sqrt{2\Phi}$, and a function $1/z$. Both curves have the same value at the ultimate limit of the calculation, 15a.u. from the jellium edge. However, the exponential graph intersects the density curve at a discrete angle, while the $1/z$ curve seems to match the asymptotic density decay. The match of the density to a $1/z$ curve is limited to a small range of less than 5a.u. Even though the vacuum density is at least three orders of magnitude higher than in standard DFT simulations, the result is therefore not fully conclusive. We shall return to this point in future publications.

4.6 Kinetic energy functionals

The potentials, energy eigenvalues, and k -values for different densities and two positions, at the center of the film, and at the peak of the surface dipole, are given in Table 3. The density, electrostatic potential, and nonlinear potential for $r_s = 1.5$ a.u. are shown in Fig. 6. The first conclusion drawn from the numerical values is that the electrostatic potential is equal to the nonlinear potential at the center of the slab. This is understandable, if one considers that the density at this point is the initial density; the product of Wigner-Seitz radius and density is in this case equal to unity. Importantly, this means that there is no correction to the electrostatic potential at this point. The situation changes at the minimum of the surface dipole potential ($z = z_0$), about 1.5a.u. from the jellium edge. Here, the charge density deviates from the initial value, and in this case the nonlinear potential will be affected. The difference, however is small and less than 10%, as the density peak does not exceed this surplus value. Concerning the eigenvalues, we find in all cases that they are equal to the potential at the center of the film. This means, that the kinetic energy density at the center of the film must be zero. A feature, which is only possible if the curvature of the wavefunctions at this point vanishes. The density oscillations at the jellium edge therefore decay into the bulk. Since the potential at the surface dipole is lower than the eigenvalue, the wavefunctions and also the densities will oscillate. Basing the oscillations, and the relation between k -values and energies of a free electron gas in a potential $v_{nl}(z_0)$, one would expect the k -values to comply with the dispersion relation:

$$\frac{1}{2}k^2 = E - v_{nl}(z_0) \quad (62)$$

r_s	$v_{el}(0)$	$v_{el}(z_0)$	$v_{nl}(0)$	$v_{nl}(z_0)$	E	$E - v_{nl}(z_0)$	k
1.5	-0.160	-0.290	-0.160	-0.265	-0.160	0.105	1.080
2.0	-0.102	-0.190	-0.102	-0.174	-0.102	0.072	0.910
2.5	-0.073	-0.136	-0.073	-0.124	-0.727	0.051	0.760
3.0	-0.056	-0.104	-0.056	-0.095	-0.556	0.039	0.660

Table 3: Potentials at the center of the film $z = 0$, at the peak of the surface dipole $z = z_0$, eigenvalue E , difference between eigenvalue and attractive potential, and wavevector k . Note that the $\frac{1}{2}k^2$ is about five times larger than the difference between eigenvalue and attractive potential at z_0 . The difference bears on the confinement of electrons, included in the kinetic energy functional (for details, see the text).

As an inspection of the numerical data shows, this is not correct. In fact, the term on the left is about five times higher than the term on the right. This means, clearly, that the kinetic energy of the nonlinear equation is not the usual single-particle or Thomas-Fermi kinetic energy. The difference becomes clear if one remembers that the fundamental change in the Schrödinger equation was dividing the kinetic single-electron term by the volume of the system. In a one-dimensional model, this corresponds to the lengthscale of the system. Here, we have to consider that the surface dipole is approximately 4-5a.u. wide: dividing the term on the left by 5 leads to the correct relation. Physically speaking, the change of the fundamental equation transformed the kinetic single-electron term into a kinetic energy functional. The decisive parameter of this functional is the confinement of the electrons in the field of the surface dipole. Regarding the energy eigenvalues it is quite clear that the energy density at the center of the slab is the same as the potential density. Approaching the jellium edge, the potential changes and the kinetic energy component changes accordingly: The system is indeed characterized by a constant energy density throughout. It is, therefore, a system in energetic equilibrium. The potential minimum between -7a.u and -3a.u. leads to an exponential decay of the wavefunction into the potential barrier and effectively screens the surface dipole from the bulk charge. This feature contains already the essence of a surface state, observed on many metal surfaces.

4.7 Summary

The method was tested for a metallic surface within a continuous background model, varying the density over a range from $r_s=1.5$ to $r_s = 3.0$ a.u. In this case we found, similarly to the results in standard DFT, that the density oscillates at the jellium edge, and that the wavelength of the oscillations depends on the jellium density. We compared the calculated eigenvalues with experimental values for the workfunctions and found good agreement, in particular in the high density range. The kinetic energy functional in the simulations includes

the confinement of electron charge. This has the effect that the energy density is constant throughout the system. Finally, we determined the decay of the density in the vacuum range. Here we find that the asymptotic behavior of the vacuum charge seems to be better described by a $1/z$ characteristic than an exponential function. In all simulations the only input parameters were the background density and the thickness of the slab.

Acknowledgements

WAH is indebted to George Darling and Jacob Gavartin for stimulating discussions, which to a large extent initiated or focussed research in this particular direction. Both authors thank Andres Arnau for sharing the jellium code, and Gilberto Teobaldi for discussions and corrections. KP is funded by the European Commission under project NMP3-CT-2004-001561. WAH thanks the Royal Society for the award of a University Research Fellowship, providing the necessary time to pursue this investigation.

References

- [1] S. Hohenberg and W. Kohn, Phys. Rev. 136, B864 (1964)
- [2] W. Kohn and L. J. Sham, Phys. Rev. 140, A1133 (1965)
- [3] R. Car and M. Parinello, Phys. Rev. Lett. 55, 2471 (1985)
- [4] E. Hernandez, M. J. Gillan, and C. M. Goringe, Phys. Rev. B 53, 7147 (1996)
- [5] W. Yang and T.-S. Lee, J. Chem. Phys. 103, 5674 (1995)
- [6] R. Baer and M. Head-Gordon, Phys. Rev. Lett. 79, 3962 (1997)
- [7] M. Levy, J.P. Perdew, and V. Sahni, Phys. Rev. A 30, 2745 (1984)
- [8] R. M. Dreizler and E. K. U. Gross, Density Functional Theory, Springer, Berlin (1990) pp.62-64
- [9] Y. A. Wang, N. Govind, and E. A. Carter, Phys. Rev. B 60, 16350 (1999)
- [10] W. A. Hofer, A. S. Foster, and A. L. Shluger, Rev. Mod. Phys. 75, 1287 (2003)
- [11] K. Palotas and W. A. Hofer, J. Phys.: Cond. Mat. 17, 2705 (2005)
- [12] S. Datta, Electronic Transport in Mesoscopic Systems, Cambridge University Press, Cambridge (1995)
- [13] W. Bao, N. J. Mauser, and H. P. Stimming, Comm. Math. Sci. 1, 909-828 (2003)

- [14] L. de Broglie, *Ann. Phys.* **3**, 22 (1925)
- [15] C. Davisson and L. H. Germer *Phys. Rev.* **30**, 705 (1927)
- [16] E. Selleri (ed.), *Quantum Mechanics versus Local Realism*, Plenum Press, New York (1988)
- [17] E. Schrödinger, *Naturwissenschaften* **23**, 807-812; 823-828; 843-848 (1935)
- [18] A. Einstein, N. Rosen, and B. Podolsky *Phys. Rev.* **47**, 180 (1935)
- [19] P. Ordejón, D. A. Drabold, M. P. Grumbach and R. M. Martin, *Phys. Rev. B* **48**, 14646 (1993); *Phys. Rev. B* **51**, 1456 (1995)
- [20] P. Pulay, *Chem. Phys. Lett.* **73**, 393 (1980)
- [21] G.P. Kerker, *J. Phys. C.: Solid St. Phys*, L189 (1980)
- [22] D. D. Johnson, *Phys. Rev. B* **38**, 12807 (1988), and references therein
- [23] R. P. Feynman, *Phys. Rev.* **56**, 340 (1939)
- [24] N. W. Ashcroft and N. D. Mermin, *Solid State Physics*, Thomson Learning (1976) p. 364
- [25] Crystallographic data were taken from <http://www.webelements.com>.
- [26] N. D. Lang and W. Kohn, *Phys. Rev B* **1**, 4555 (1970)
- [27] N. D. Lang and W. Kohn, *Phys. Rev. B* **3**, 1215 (1971)
- [28] J. L. M. Quiroz Gonzalez and D. Thompson, *Computers in Physics* **11**, 514 (1997)
- [29] W. A. Hofer, PhD thesis, Technische Universität Wien (1999)

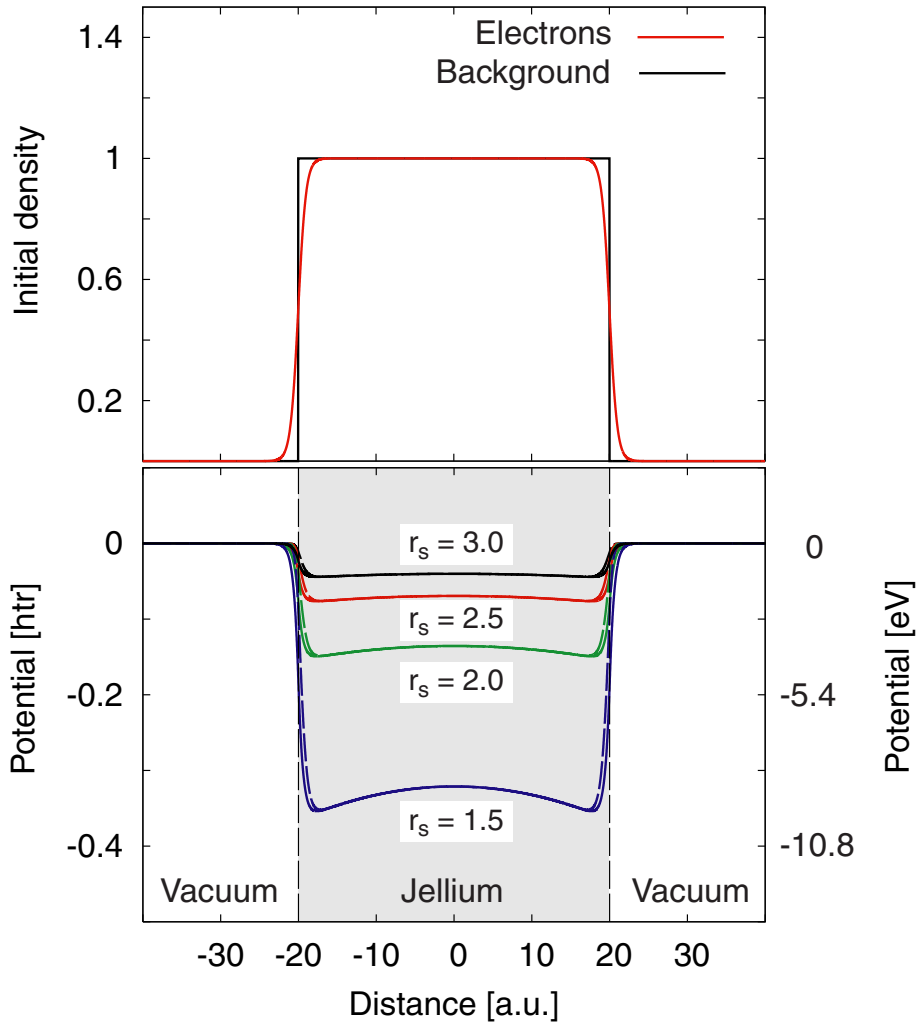


Figure 1: (Color online) Setup for the calculation of metal surfaces. The jellium film is embedded in two vacuum ranges (top). The initial electrostatic potential (full graphs) inside the slab is equal to the non-linear potential (dashed graphs) as defined in Eq. 58. The potential varies with the density of the background (bottom).

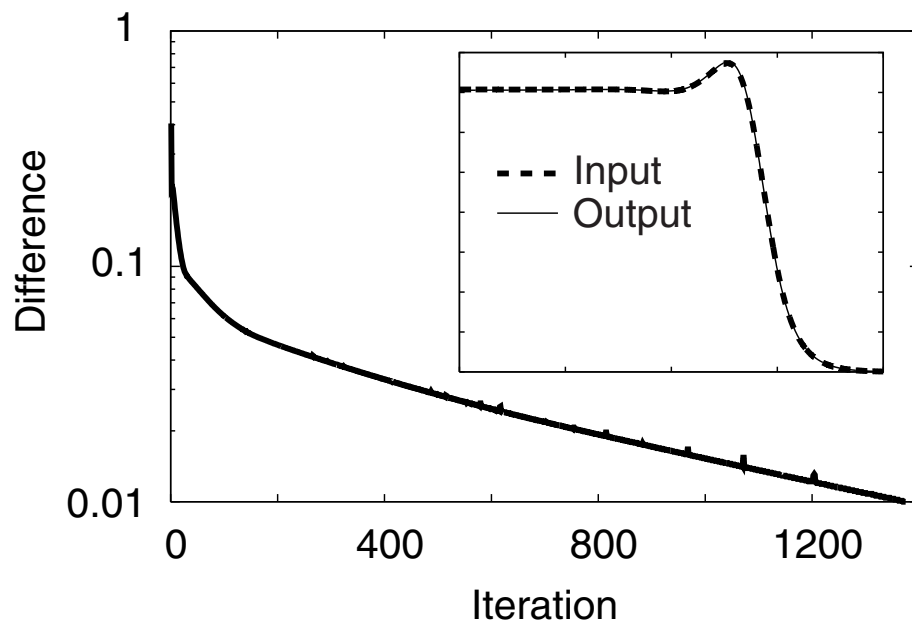


Figure 2: Convergency of the iterations. The difference between input and output charge density decreases close to exponentially to its final value below 0.01. In the final iteration input and output charge density are identical (inset).

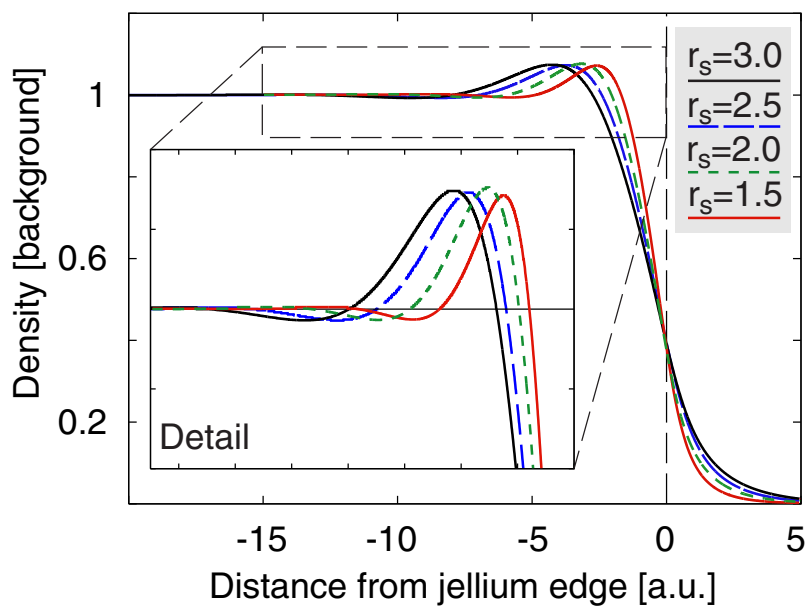


Figure 3: (Color online) Density oscillations at the jellium edge. The density shows a characteristic peak at the boundary. The maximum value of the density is nearly equivalent in all simulations and about 8% higher than the density of positive charge. The oscillations decay into the bulk, the characteristic wavelength decreases with increasing density (see detail).

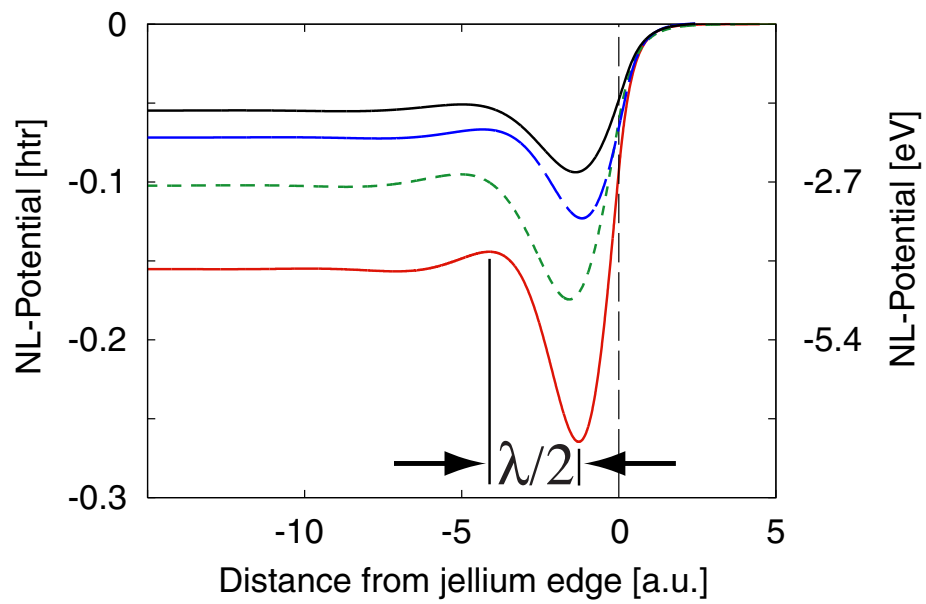


Figure 4: (Color online) Non-linear potential of the fully converged systems. The surface dipole corresponds to a minimum of the potential near the jellium edge. The characteristic wavelength λ decreases with increasing density.

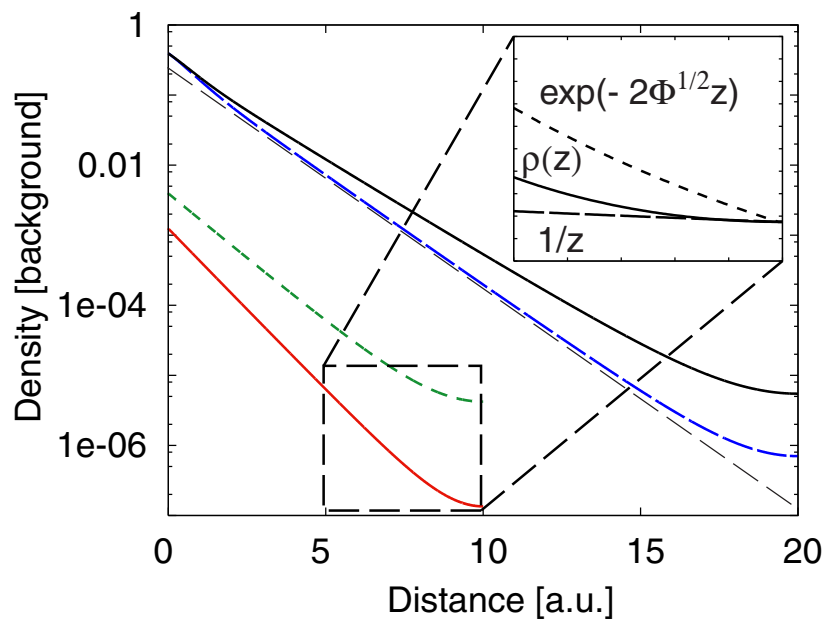


Figure 5: (Color online) Density decay in the vacuum region. The logarithmic plot shows a substantial deviation from an exponential behavior in the high distance regime.

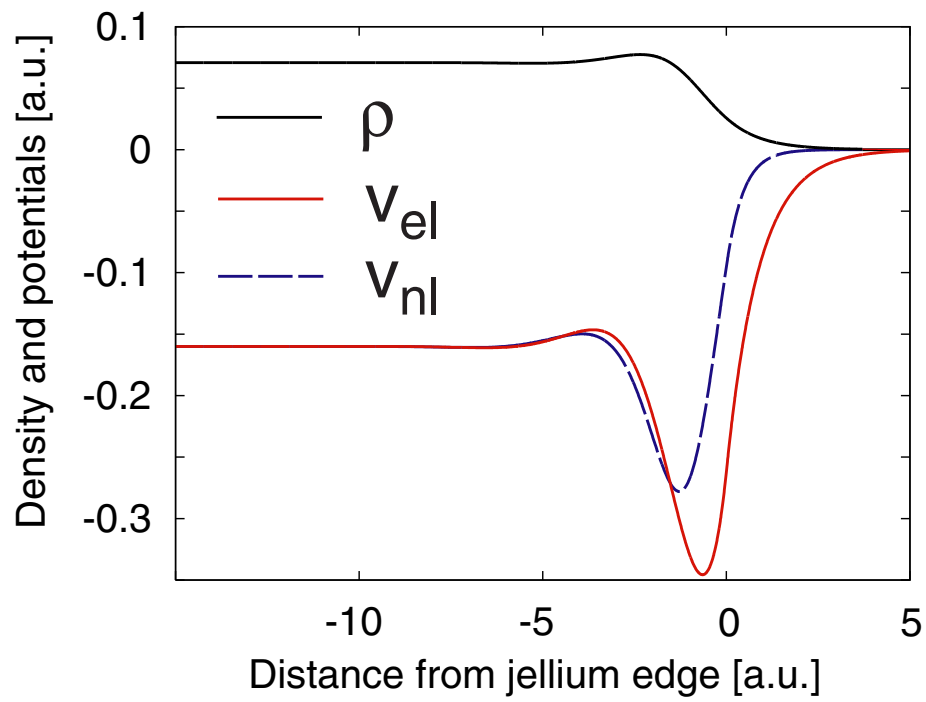


Figure 6: (Color online) Density, electrostatic potential, and nonlinear potential for $r_s = 1.5$ a.u. The potential barrier around -4 a.u. screens surface electrons from bulk electrons.